

# Exotic Shapes in $^{32}\text{S}$ suggested by the Symmetry-Unrestricted Cranked Hartree-Fock Calculations <sup>1</sup>

Masayuki Yamagami and Kenichi Matsuyanagi

*Department of Physics, Graduate School of Science, Kyoto University,  
Kitashirakawa, Kyoto 606-8502, Japan*

## Abstract.

High-spin structure of  $^{32}\text{S}$  is investigated by means of the cranked Skyrme-Hartree-Fock method in the three-dimensional Cartesian-mesh representation. Some interesting suggestions are obtained: 1) An internal structure change (toward hyperdeformation) may occur at  $I > 20$  in the superdeformed band, 2) A non-axial  $Y_{31}$  deformed band may appear in the yrast line with  $5 \leq I \leq 13$ .

## Introduction

Since the discovery of the superdeformed(SD) band in  $^{152}\text{Dy}$ , about two hundreds SD bands have been found in various mass ( $A=60, 80, 130, 150, 190$ ) regions [1]. Yet, the doubly magic SD band in  $^{32}\text{S}$ , which has been expected quite a long time [2,3] remains unexplored, and will become a great challenge in the coming years.

Quite recently, we have constructed a new computer code for the cranked Skyrme Hartree-Fock (HF) calculation based on the three-dimensional (3D) Cartesian-mesh representation, which provides a powerful tool for exploring exotic shapes (breaking both axial and reflection symmetries in the intrinsic states) at high spin in unstable nuclei as well as in stable nuclei. As a first application of this new code, we have investigated high-spin structure of  $^{32}\text{S}$  and obtained some interesting results on which we are going to discuss below.

## Cranked Skyrme HF Calculation

We solve the cranked HF equation

$$\delta \langle H - \omega_{rot} J_x \rangle = 0 \quad (1)$$

in the 3D Cartesian-mesh representation. We adopt the standard algorithm [4-7] but completely remove various restrictions on spatial symmetries. When we allow for the simultaneous breaking of both reflection and axial symmetries, it is crucial to fulfill the center-of-mass condition

$$\langle \sum_{i=1}^A x_i \rangle = \langle \sum_{i=1}^A y_i \rangle = \langle \sum_{i=1}^A z_i \rangle = 0, \quad (2)$$

and the principal-axis condition

$$\langle \sum_{i=1}^A x_i y_i \rangle = \langle \sum_{i=1}^A y_i z_i \rangle = \langle \sum_{i=1}^A z_i x_i \rangle = 0. \quad (3)$$

---

<sup>1)</sup> Talk presented by K.M. at the *Nuclear Structure '98* International Conference, August 10-15, 1998, Gatlinburg, Tennessee.

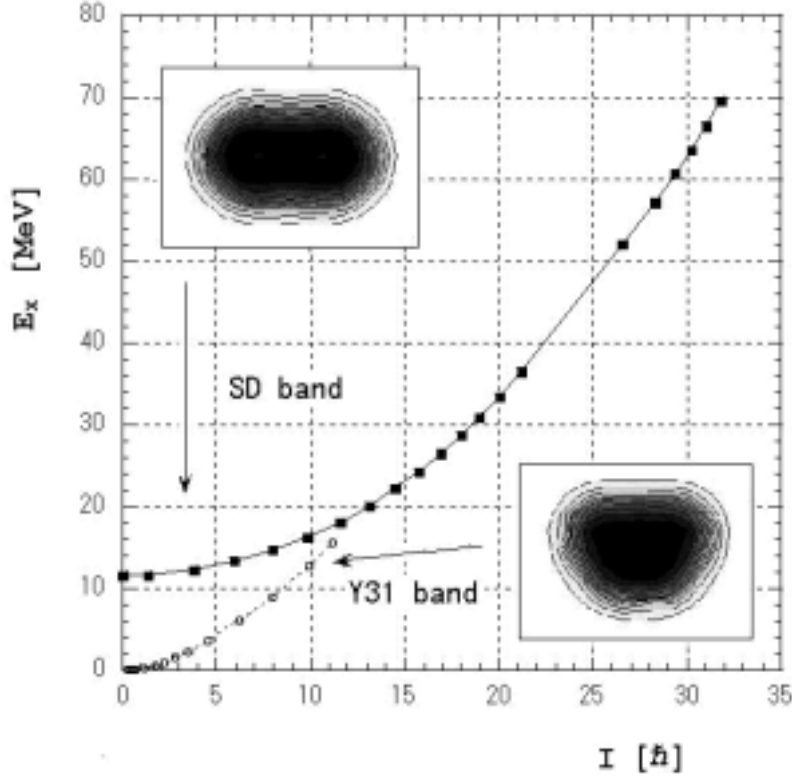


**FIGURE 1.** Excitation energy versus angular-momentum plot of the yrast structure of  $^{32}\text{S}$  calculated with the Skyrme III interaction. Density distributions projected on the plane perpendicular to the rotation axis are shown, as insets, for the SD band (solid line with filled squares), and the  $Y_{31}$  band (broken line with open circles).

Special care is taken to accurately fulfill the above conditions during the iteration procedure. We solve these equations inside the sphere with radius  $R=8[\text{fm}]$  and mesh size  $h=1[\text{fm}]$ , starting with various initial configurations. We use the Skyrme III interaction which has been successful in describing systematically the ground-state quadrupole deformations in a wide area of nuclear chart [7]. Results of the calculation are presented in Figs. 1-3. Figure 1 shows the structure of the yrast line. The expected superdeformed(SD) band becomes the yrast for  $I \geq 14$ . In addition to the SD band, we obtained an interesting band possessing the  $Y_{31}$  deformation, which appears in the yrast line with  $5 \leq I \leq 13$ . Let us call this band “ $Y_{31}$  band.” The calculated angular momentum  $I$  and deformation  $\delta$  for the SD band and the  $Y_{31}$  band are shown in Figs. 2 and 3 as functions of the rotational frequency  $\omega_{rot}$ . Below we shall first discuss the SD band and then about the  $Y_{31}$  band.

### High-Spin Limit of the Superdeformed Band

The SD band is obtained from  $I = 0$  to about  $I = 20\hbar$ . The potential energy surface for the SD state at  $I = 0$  is shown in Fig. 4. We see that the excitation energy of the SD state at  $I = 0$  is about 12 MeV.<sup>2</sup> It becomes the yrast above  $I = 14\hbar$ .

A particularly interesting point is the behavior of the SD band in the high-spin limit: It is clearly seen in

<sup>2)</sup> The rotational zero-point energy corrections are evaluated to be -4.3 MeV and -1.1 MeV for the SD and the ground-state configurations, respectively. If we take these corrections into account, the excitation energy becomes about 9 MeV.

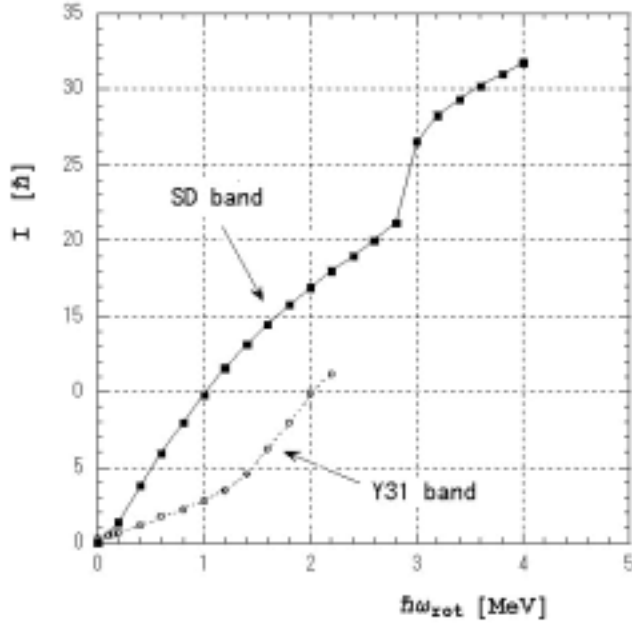


**FIGURE 2.** Angular momenta  $I$  plotted as a function of the rotation frequency  $\omega_{rot}$  for the SD band (solid line with filled squares) and the  $Y_{31}$  band (broken line with open circles).

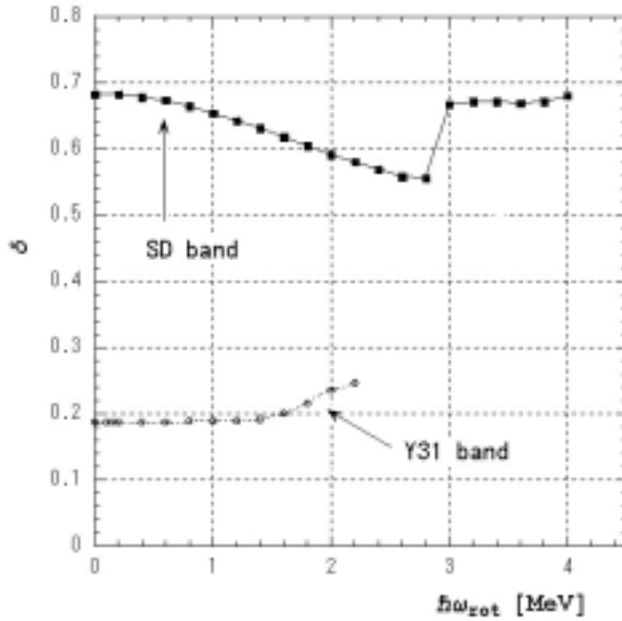


**FIGURE 3.** Deformation  $\delta$  plotted as a function of the rotation frequency  $\omega_{rot}$  for the SD band (solid line with filled squares) and the  $Y_{31}$  band (broken line with open circles).  $\delta$  is defined as  $\delta = \frac{3}{4} \frac{\langle \sum_{i=1}^A (2x_i^2 - y_i^2 - z_i^2) \rangle}{\langle \sum_{i=1}^A (x_i^2 + y_i^2 + z_i^2) \rangle}$ .

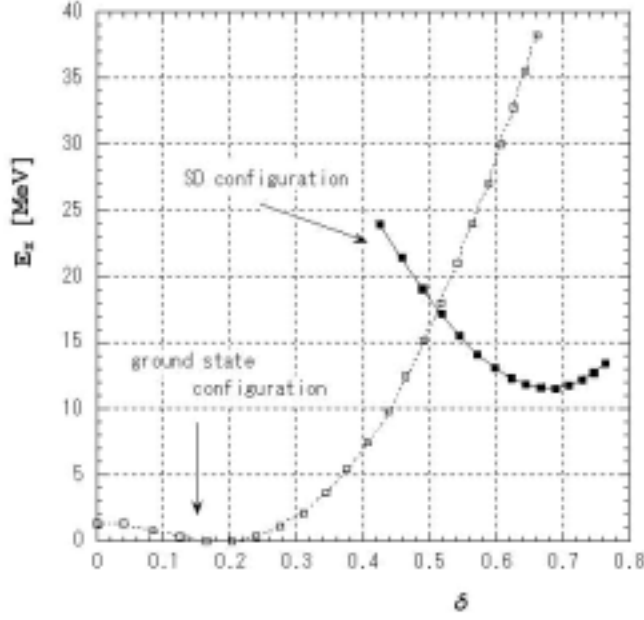


**FIGURE 4.** Potential energy surface for the SD configuration at  $I = 0$  (solid line with filled squares) relative to that for the ground state configuration (dotted line with open squares). This calculation was done by means of the constrained HF procedure [8].

Figs. 2 and 3 that a jump occurs both in the angular momentum  $I$  and the deformation  $\delta$  at  $\omega_{rot} \simeq 3 \text{ MeV}/\hbar$ . At this point,  $I$  jumps from about  $22$  to  $26\hbar$ , and  $\delta$  increases from about  $0.56$  to  $0.66$ . This is due to the level crossing with the rotation-aligned  $[440]_{\frac{1}{2}}$  orbit. Thus the states above  $I \simeq 24\hbar$  may be better characterized as the hyperdeformed configuration rather than the SD configuration. Such a singular behavior of the SD band can be noticed also in the previous cranked HF calculation with the BKN force [9], but no explanation of its microscopic origin was given there. Let us note that if we regard the SD configuration as to correspond to the  $j$ - $j$ -coupling shell model  $4p$ - $12h$  configuration  $\pi[(f_{7/2})^2(sd)^{-6}] \otimes \nu[(f_{7/2})^2(sd)^{-6}]$  (relative to  $^{40}\text{Ca}$ ) in the spherical limit, the maximum angular momentum that can be generated by aligning the single-particle angular momenta toward the direction of the rotation axis is  $24\hbar$ , and thus “the SD band termination” may be expected at this angular momentum. Interestingly, our calculation suggests that a crossover to the hyperdeformed band takes place just at this region of the yrast line.

## Effects of Time-Odd Components

It would be interesting to examine the effect of rotation-induced time-odd components in the mean field. In Fig. 5 we compare the results of calculation with and without the time-odd components. From this figure we can easily confirm that the dynamical moment of inertia  $J^{(2)} = \partial I / \partial \omega_{rot}$  of the SD band increases about 30% due to the time-odd components. This increase is well compared with the effective-mass ratio  $m/m^* = 1/0.76 \simeq 1.3$  for the Skyrme III interaction, and seems to be consistent with what expected from the restoration of the local Galilean invariance [10] (more generally speaking, local gauge invariance [11]) of the Skyrme force; namely, the major effect of the time-odd components is to restore the decrease of the moment of inertia due to the effective mass  $m^*$  and bring it back to the value for the nucleon mass  $m$ .

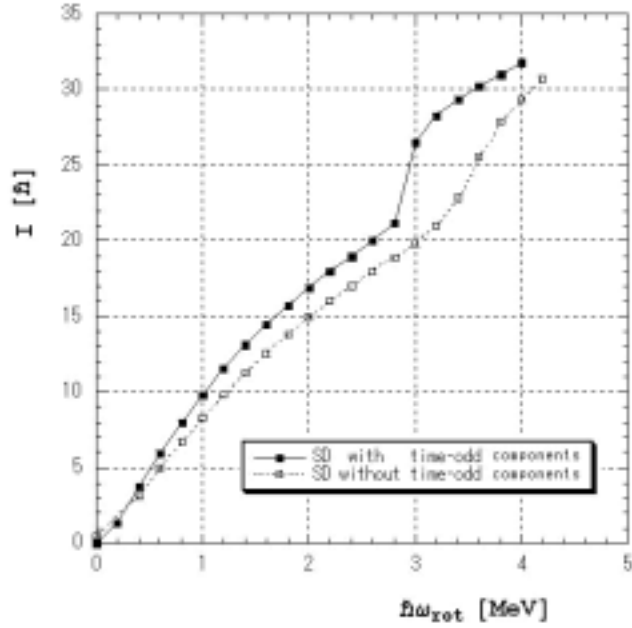


**FIGURE 5.** Angular momenta  $I$  of the SD band plotted as a function of the rotation frequency  $\omega_{rot}$ . The solid line with filled squares (dotted line with open squares) indicates the result with (without) the time-odd components.

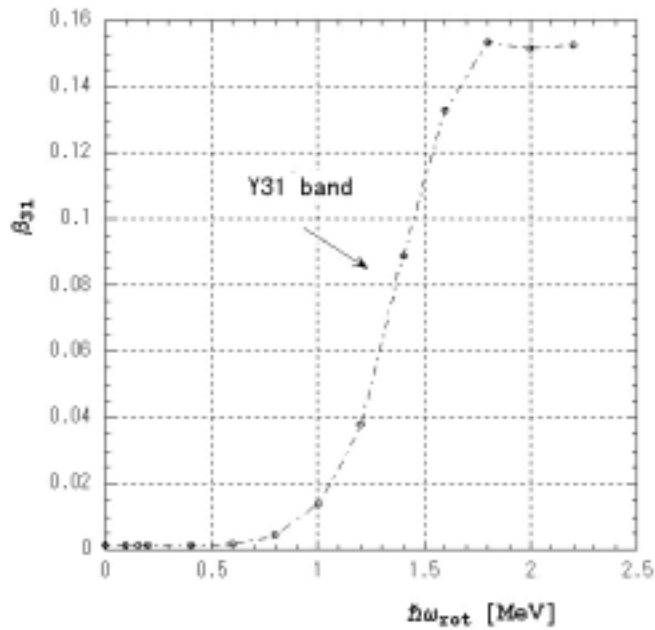


**FIGURE 6.** Non-axial octupole deformation  $\beta_{31}$  of the  $Y_{31}$  band, plotted as a function of the rotation frequency  $\omega_{rot}$ .  $\beta_{31}$  is defined through the mass-octupole moments in the usual manner .

## $Y_{31}$ Deformation

As noticed in Fig. 1, we found that a non-axial  $Y_{31}$  deformed band ( $\delta \simeq 0.2$  and  $\beta_{31} = 0.1 \sim 0.15$ ) appears in the yrast line with  $5 \leq I \leq 13$ . It should be emphasized that this band does not exist at  $I = 0$  but emerges at high spin: As shown in Fig. 6, the  $Y_{31}$  deformation quickly rises when  $\omega_{rot}$  exceeds  $1 \text{ MeV}/\hbar$ .

Formation mechanism of this band is well described as a function of angular momentum  $I$  by means of the new cranked HF code allowing for the simultaneous breaking of both axial and reflection symmetries. We found that this band emerges as a result of the strong coupling between the rotation-aligned  $[330]_{\frac{1}{2}}$  orbit and the  $[211]_{\frac{1}{2}}$  orbit. The matrix element of the  $Y_{31}$  operator between these single-particle states is large, since they satisfy the selection rule for the asymptotic quantum numbers ( $\Delta\Lambda = 1, \Delta n_z = 2$ ).

## Conclusions

We have investigated high-spin structure of  $^{32}\text{S}$  by means of the cranked Skyrme HF method in the 3D Cartesian-mesh representation, and suggested that

- 1) an internal structure change (toward hyperdeformation) may occur at  $I > 20$  in the superdeformed band,
- 2) a non-axial  $Y_{31}$  deformed band may appear in the yrast line with  $5 \leq I \leq 13$ .

We have obtained similar results also in calculations with the Skyrme  $M^*$  interaction. More detailed study including dependence on effective interactions is in progress.

## REFERENCES

1. Dobaczewski J., contribution to this conference.
2. Sheline R.K., Ragnarsson L., and Nilsson S.G., *Phys. Lett.* **41B**, 115(1972).
3. Leander G., and Larsson S.E., *Nucl. Phys.* **A239**, 93 (1975).
4. Davies K.T.R., Flocard H., Krieger S.J., and Weiss M.S., *Nucl. Phys.* **A342**, 111(1980).
5. Bonche P., Flocard H., Heenen P.H., Krieger S.J., and Weiss M.S., *Nucl. Phys.* **A443**, 39(1985).
6. Bonche P., Flocard H., Heenen P.H., *Nucl. Phys.* **A467**, 115(1987).
7. Tajima N., Takahara S., and Onishi N., *Nucl. Phys.* **A603**, 23(1996).
8. Flocard H., Quentin P., Kerman A.K., and Vautherin D., *Nucl. Phys.* **A203**, 433(1973).
9. Flocard H., Heenen P.H., Krieger S.J., and Weiss M.S., *Prog. Theor. Phys.* **72**, 1000(1984).
10. Bohr A., and Mottelson B.R., *Nuclear Structure*: Benjamin, 1975, Vol. 2.
11. Dobaczewski J., and Dudek J., *Phys. Rev.* **C52**, 1827(1995).